ON THE INFLUENCE OF ANTI-ROLL STIFFNESS ON VEHICLE STABILITY AND PROPOSAL OF AN INNOVATIVE SEMI-ACTI....

Conference Paper · September 2012

CITATIONS
5

READS
1,299

5 authors, including:

Flavio Farroni
University of Naples Federico II
33 PUBLICATIONS **160** CITATIONS
SEE PROFILE

Riccardo Russo
University of Naples Federico II
58 PUBLICATIONS **594** CITATIONS
SEE PROFILE

Mario Terzo
University of Naples Federico II
76 PUBLICATIONS **445** CITATIONS
SEE PROFILE

Francesco Timpone
University of Naples Federico II
53 PUBLICATIONS **254** CITATIONS
SEE PROFILE

Proceedings of the RAAD 2012
21th International Workshop on Robotics in Alpe-Adria-Danube Region
September 10-13, 2012, Napoli, Italy

ON THE INFLUENCE OF ANTI-ROLL STIFFNESS ON VEHICLE STABILITY AND PROPOSAL OF AN INNOVATIVE SEMI-ACTIVE MAGNETORHEOLOGICAL FLUID ANTI-ROLL BAR

Flavio Farroni, Michele Russo, Riccardo Russo, Mario Terzo and Francesco Timpone

Dipartimento di Meccanica ed Energetica, University of Naples "Federico II"- Napoli, Italy
E-mail: flavio.farroni@unina.it

Abstract. Modern vehicles are equipped with several active and passive devices whose function is to increase active safety. This paper is focused on the anti-roll stiffness influence on vehicle handling, and follows a theoretical approach.
The work firstly develops a quadricycle theoretical model, useful to study the influence of anti-roll stiffness on the vehicle local stability. The model, involving non-linear phenomena, is simplified by proper linearizations.
This procedure allows local stability analysis with low computational load. At the same time, the linearized model takes into account the dynamic effects induced by load transfers through a tyre-road interaction model sensitive to the vertical load. The study is conducted considering the anti-roll stiffnesses of the two axles as parameters. The proposed model defines the relationship between the anti-roll bars stiffness and the system state.
In order to realize an adaptive system able to provide a variable roll stiffness, a semi-active anti-roll bar prototype, employing magnetorheological fluid, is described. Such device gives the possibility to quickly change the roll stiffness, according to the system state, to preserve its stability.

Keywords. Vehicle Dynamics, Local Stability, Anti-Roll Stiffness, Magnetorheological Fluid.

1. Introduction

In recent years, the interest for vehicle stability control systems has been increasing, and consequently the study of the local stability has become a fundamental discipline in the field of vehicle dynamics.
Loss of stability of a road vehicle in the lateral direction may result from unexpected lateral disturbances like side wind force, tyre pressure loss, or μ-split braking due to different road pavements such as icy, wet, and dry pavement. During short-term emergency situations, the average driver may exhibit panic reaction and control authority failure, and he may not generate adequate steering, braking/throttle commands in very short time periods. Vehicle lateral stability control systems may compensate the driver during panic reaction time by generating the necessary corrective yaw moments.

The main idea of this paper is to approach the local stability analysis in a simplified way, taking into account all the phenomena involved in the lateral vehicle dynamics. In particular, the adopted tyre model is the Pacejka magic formula, which has been linearized around a steady-state vehicle equilibrium point, expressing the lateral force as a function of both slip angle and vertical load. This kind of linearization allows to take also into consideration the tyre saturation behaviour with respect to the vertical load.
The adopted vehicle model is an 8-DOF quadrycicle planar model performing a reference manoeuvre chosen with the aim to consider the lateral vehicle dynamics.
The study of local stability has been addressed by analyzing the state matrix of the linearized motion equations in matrix form.
This analysis shows the influence of anti-roll stiffness on local vehicle stability and the importance of a

proper variation of its value to preserve vehicle safety conditions.
At the end of the work an innovative semi-active anti-roll bar is described. In particular, it is able to vary axle anti-roll stiffness according to vehicle dynamics conditions in order to guarantee stability and handling.

2. Vehicle model

The vehicle has been modelled using an 8 degree-of-freedom quadricycle planar model. In particular, 3 DOF refer to in plane vehicle body motions (longitudinal, lateral and jaw motions), 4 DOF to wheel rotations and the last DOF to the steering angle. To describe the vehicle motions two coordinate systems have been introduced: one earth-fixed (X' ; Y'), the other (x ; y) integral to the vehicle as shown in Fig. 1.
With reference to the same figure, v is the centre of gravity absolute velocity referred to the earth-fixed axis system and U (longitudinal velocity) and V (lateral velocity) are its components in the vehicle axis system; r is the jaw rate evaluated in the earth fixed system, β is the vehicle sideslip angle, F_{xi} and F_{yi} are respectively longitudinal and lateral components of the tyre-road interaction forces.
The wheel track is indicated with t and it is supposed to be the same for front and rear axle; the distances from front and rear axle to the centre of gravity are represented by a and b, respectively. The steer angle of the front tyres is denoted by δ, while the rear tyres are supposed non-steering.

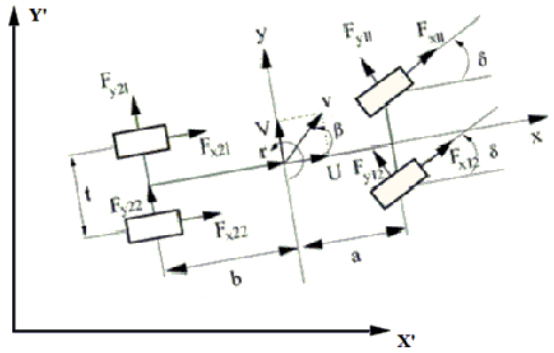

Fig. 1. Coordinate systems.

In hypothesis of negligible aerodynamic interactions, little steer angles (<15°) and rear wheel drive, the motion equations of in plane vehicle dynamics (Guiggiani, 2007) are:

$$\begin{aligned} m(\dot{U} - Vr) &= (F_{x_{21}} + F_{x_{22}}) - (F_{y_{11}} + F_{y_{12}})\delta \\ m(\dot{V} + Ur) &= F_{y_{11}} + F_{y_{12}} + F_{y_{21}} + F_{y_{22}} \\ J_z\dot{r} &= (F_{y_{11}} + F_{y_{12}})a - (F_{y_{21}} + F_{y_{22}})b - (F_{x_{21}} - F_{x_{22}})\frac{t}{2} + (F_{y_{11}} \\ &\quad - F_{y_{12}})\,\delta\frac{t}{2} \end{aligned} \tag{1}$$

where m is the vehicle total mass and J_z is its moment of inertia with respect to z axis

2.1. Manoeuvre

The simulation scenario is described as a curve to the left, approached with an increasing steering law, described by a sinusoid between 0 and π/2; the torque M_m, transmitted to the rear wheels, increases with the same kind of function. This kind of input-laws have been chosen with the aim of not generating irregularities in the simulation; it allows to reach the steady state with a signal that shows null derivative values in the origin and at the end of the transient state.
At the end of the described manoeuvre, defined henceforth as "reference manoeuvre", the vehicle reaches an equilibrium condition, characterized by constant values of the physical quantities. This equilibrium state, once determined, represents the point in whose neighbourhood will be analyzed the system in the space state.

2.2. Wheel motion dynamics

Angular velocities are calculated integrating the angular accelerations $\dot{\omega}_{ij}$, obtained thanks to wheel dynamics equation:

$$I_{w_{ij}}\dot{\omega}_{ij} = M_{m_{ij}} - F_{x_{ij}}R \tag{2}$$

where I_w is wheel moment of inertia with reference to its revolution axis, $\dot{\omega}_{ij}$ are the tyre angular accelerations and R is the tyre effective radius.
The longitudinal wheel slip ratios are given by:

$$\begin{aligned} s_{11} &= \frac{\left(U - r\frac{t}{2}\right)\cos(\delta) + (V + ra)\sin(\delta) - \omega_{11}R}{\omega_{11}R} \\ s_{12} &= \frac{\left(U + r\frac{t}{2}\right)\cos(\delta) + (V + ra)\sin(\delta) - \omega_{12}R}{\omega_{12}R} \\ s_{21} &= \frac{\left(U - r\frac{t}{2}\right)\cos(0) - (V - rb)\sin(0) - \omega_{21}R}{\omega_{21}R} \\ s_{22} &= \frac{\left(U + r\frac{t}{2}\right)\cos(0) - (V - rb)\sin(0) - \omega_{22}R}{\omega_{22}R} \end{aligned} \tag{3}$$

in which ω_{ij} are the tyre angular velocities. For little steering angles and not-steering rear tyres, last equations become:

$$\begin{aligned} s_{11} &= \frac{\left(U - r\frac{t}{2}\right) + (V + ra)\delta - \omega_{11}R}{\omega_{11}R} \\ s_{12} &= \frac{\left(U + r\frac{t}{2}\right) + (V + ra)\delta - \omega_{12}R}{\omega_{12}R} \\ s_{21} &= \frac{\left(U - r\frac{t}{2}\right) - \omega_{21}R}{\omega_{21}R} \\ s_{22} &= \frac{\left(U + r\frac{t}{2}\right) - \omega_{22}R}{\omega_{22}R} \end{aligned} \tag{4}$$

2.3. Tyre model

One of the most critical aspects in modelling the dynamics of a vehicle is the determination of the lateral force generated by the interaction between tyre and road. The underlying physical phenomenon is rather complex and, for its description, is often necessary referring to empirical models, the most renowned of which is undoubtedly the Pacejka's magic formula (Pacejka, 2005, Garatti and Bittanti, 2009).

This allows the expression of the lateral force as a function of the slip angle α and of the vertical load F_z by means of a non-linear function. The formula contains a number of parameters, the value of which has to be tuned in order to distinguish between different kinds of tyres, with their own characteristics in terms of size, constitutive material, inflation pressure, etc.

In the Pacejka's magic formula, parameters have no clear physical meaning, and usually they are estimated from experimental data. In the present work the parameters are referred to a common passenger tyre.

With reference to the described quadricycle model (Guiggiani, 2007) the slip angles are:

$$\begin{aligned} \alpha_{11} &= \delta - tan^{-1}\left(\frac{V + ra}{U - r\frac{t}{2}}\right) \\ \alpha_{12} &= \delta - tan^{-1}\left(\frac{V + ra}{U + r\frac{t}{2}}\right) \\ \alpha_{21} &= -tan^{-1}\left(\frac{V - rb}{U - r\frac{t}{2}}\right) \\ \alpha_{22} &= -tan^{-1}\left(\frac{V - rb}{U + r\frac{t}{2}}\right) \end{aligned} \tag{5}$$

With reference to the reached steady state conditions of a curving manoeuvre, it is possible to neglect the low longitudinal load transfers due to the lateral interaction forces and so the attention can be focused on these last and on the lateral load transfers.

The non-linear tyre Pacejka model, coupled with the vehicle model, is employed to determine the steady-state conditions in the neighborhood of which the analysis of the influence of the anti-roll stiffness on vehicle stability is carried out.

In order to execute the local stability analysis and to evaluate the influence of the anti-roll stiffness, it is necessary to take into account the saturation of the lateral interaction with respect to vertical load. At the same time, vehicle and interaction models have to be as simple as possible in order to express them in a state space form. In this way, the local stability analysis can be executed via state matrix eigenvalues calculus.

To this aim, the proposed model is characterized by a linearization of lateral force with respect to slip angle α and vertical load F_z around the reached steady state conditions. In fact, once determined the steady state conditions (i.e. known the equilibrium point) for each tyre, a linearization of the lateral force is executed with respect to slip angle and vertical load. Consequently, tyre-road interaction will consist in a linear relation for each tyre.

The linearization process of the lateral forces modeled by Pacejka in the neighbourhood of the working point consists of the identification of three parameters (m_{1ij}, m_{2ij}, q_{ij}, different for each tyre), necessary to set a linear relationship expressing the lateral force as a function of vertical load and slip angle.

So, the proposed generic lateral force F_{yij} expression will be:

$$F_{y_{ij}} = (m_{1_{ij}} F_{z_{ij}} + q_{ij}) + m_{2_{ij}} \alpha_{ij} \tag{6}$$

where the term in parenthesis, dependent on the vertical load, can be seen as the bias of the expression related to the slip angle.

As an example, in Fig. 2 and 3 the results of the double linearization are shown as concerns the left front tyre. Particularly, Fig. 2 illustrates, for the steady state vertical load (F_{zss}), Pacejka relationship between F_y and α (continuous curve) and its linearization (dotted curve) around the steady-state point. Fig. 3 shows linearization with respect to vertical load for the steady-state α value (α_{ss}).

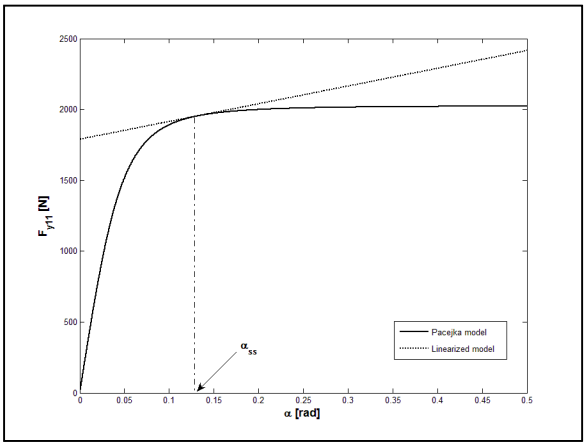

Fig. 2. Result of the linearization of Pacejka model in an α - F_y plane for $F_z = F_{zss}$

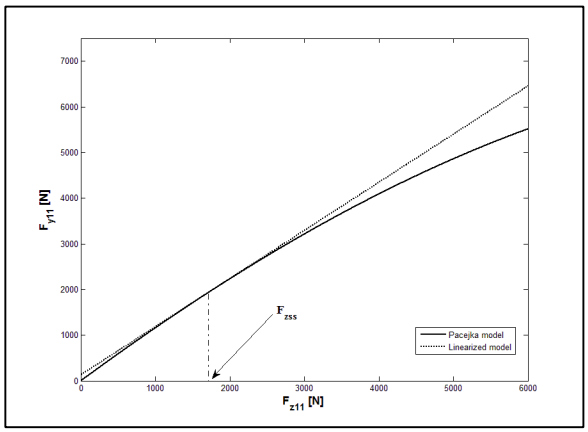

Fig. 3. Result of the linearization of Pacejka model in an F_z - F_y plane for $\alpha = \alpha_{ss}$

The proposed linearized model allows to take into account the effects of the lateral forces with respect to the vertical load saturation due to the lateral load transfers. The different angular coefficients characterizing each tangent to the $F_z - F_y$ curve in the working point allows to well approximate this phenomenon.

Ignoring camber angles and aligning moments, the normal forces take into account the lateral load transfers as follows (Guiggiani, 2007):

$$
\begin{aligned}
F_{z_{11}} &= \frac{mGb}{2(a+b)} - \frac{1}{t}\left[d(F_{y_{11}} + F_{y_{12}}) + \frac{k_{\phi_1}}{k_\phi}(h-d)(F_{y_{11}} + F_{y_{12}} + F_{y_{21}} + F_{y_{22}})\right] \\
F_{z_{12}} &= \frac{mGb}{2(a+b)} + \frac{1}{t}\left[d(F_{y_{11}} + F_{y_{12}}) + \frac{k_{\phi_1}}{k_\phi}(h-d)(F_{y_{11}} + F_{y_{12}} + F_{y_{21}} + F_{y_{22}})\right] \\
F_{z_{21}} &= \frac{mGa}{2(a+b)} - \frac{1}{t}\left[d(F_{y_{21}} + F_{y_{22}}) + \frac{k_{\phi_2}}{k_\phi}(h-d)(F_{y_{11}} + F_{y_{12}} + F_{y_{21}} + F_{y_{22}})\right] \\
F_{z_{22}} &= \frac{mGa}{2(a+b)} + \frac{1}{t}\left[d(F_{y_{21}} + F_{y_{22}}) + \frac{k_{\phi_2}}{k_\phi}(h-d)(F_{y_{11}} + F_{y_{12}} + F_{y_{21}} + F_{y_{22}})\right]
\end{aligned}
\tag{7}
$$

where G is the gravity acceleration, d is the height of the intersection point between the roll-axis and the vertical plane passing by y-axis, h is the height of the centre of gravity, k_{ϕ_1} and k_{ϕ_2} are, respectively, front and rear axle anti-roll stiffnesses and their sum is indicated with $k_\phi = k_{\phi_1} + k_{\phi_2}$.

3. Motion equations and local stability analysis

According to the theory of dynamic systems, the steady motion of a vehicle constitutes an equilibrium point for the state variables. The local stability analysis of a dynamic system around an equilibrium point involves the eigenvalue analysis of the corresponding linearized equations of motion.

For a rear wheel drive vehicle with no steering rear wheels, the motion system of equations simplifies to an extreme degree, being composed by only two differential equations in V(t) and r(t), in which the forces F_z and F_y have been calculated in Eq. 6 and 7 (Guiggiani, 2007).

The terms $(F_{x_{21}} - F_{x_{22}})\frac{t}{2}$ and $(F_{y_{11}} - F_{y_{12}})\,\delta\frac{t}{2}$, appearing in motion equations (Eq. 1), can be neglected; the first one is null for vehicles equipped with an ordinary open differential, the second one is neglectable for its low value:

$$
\begin{aligned}
m(\dot{V} + Ur) &= F_{y_{11}} + F_{y_{12}} + F_{y_{21}} + F_{y_{22}} \\
J_z\dot{r} &= (F_{y_{11}} + F_{y_{12}})a - (F_{y_{21}} + F_{y_{22}})b
\end{aligned}
\tag{8}
$$

that, expliciting the derivatives of the state variables, become:

$$
\begin{aligned}
\dot{V} &= \frac{F_{y_{11}} + F_{y_{12}} + F_{y_{21}} + F_{y_{22}}}{m} - Ur \\
\dot{r} &= \frac{(F_{y_{11}} + F_{y_{12}})a - (F_{y_{21}} + F_{y_{22}})b}{J_z}
\end{aligned}
\tag{9}
$$

Solving the system in function of r and V allows to obtain the equilibrium values of these variables (r_p, V_p). The validity of the linearization process previously described is confirmed by the correspondence between the values of r_p and V_p and the values of the same variables (r* and V*) calculated at the steady state conditions reached below for the reference manoeuvre with the complete vehicle model.

The calculation of the values of the state variables in the equilibrium conditions (r_p, V_p) is necessary for the expression of the motion equations as a Taylor series. Arresting the calculation at the first order, the system of equations of motion can be written in matrix notation and its solution needs to be evaluated numerically (Escalona and Chamorro, 2007):

$$\dot{w} = Aw + k \tag{10}$$

where w(t)=(V(t), r(t)) is the state variables vector, A is the state matrix and k is the constant terms vector.

If U=constant (and this condition is satisfied by the reached steady state) the system becomes a constant coefficients linear system. It allows to solve analytically the homogeneous system:

$$\dot{w}_0 = Aw_0 \tag{11}$$

The eigenvalues λ_1 and λ_2 can be calculated thanks to the equation:

$$\det(A - \lambda I) = 0 \tag{12}$$

and are linked with tr(A) and det(A) with the following relations:

$$tr(A) = \lambda_1 + \lambda_2$$
$$\det(A) = \lambda_1 \lambda_2 \quad (13)$$

Vehicle stability is determined by λ_1 and λ_2, and, more precisely, by their real parts $Re(\lambda_1)$ and $Re(\lambda_2)$. The system is asymptotically stable around its equilibrium point if its eigenvalues have negative real part:

$$stability \Leftrightarrow Re(\lambda_1) < 0 \; and \; Re(\lambda_2) < 0 \quad (14)$$

The just defined real parts are called Lyapunov exponents, but stability can be studied directly referring to the trace and to the determinant of the state matrix. The conditions to satisfy are:

$$stability \Leftrightarrow tr(A) < 0 \; and \; det(A) > 0 \quad (15)$$

The linearizations operated in the model allow to decrease the computational loads required to solve the motion equations expliciting $\dot{V}$ and $\dot{r}$ and consequentially make possible the study of the trace and of the determinant of the state matrix.

4. Results

The vehicle model simulations results are presented in this section, highlighting the influence of anti-roll stiffness on vehicle stability. In particular, the simulations have been carried on varying the anti-roll stiffness of the only front axle.

Fig. 4 illustrates det(A) with respect to tr(A) variations for different constant values of front anti-roll stiffness, for a constant-steering curving manoeuvre, performed at increasing U. It shows how, varying properly the bar stiffness, it is possible to reach more stable equilibrium configurations, expressed by higher values of det(A). Moreover, it can be noticed that the manoeuvres characterized by the same values of steering angle and longitudinal velocity, (indicated in the plot by the marked points), represent more stable equilibrium configurations for higher values of the anti-roll stiffness, showing the relevance of this parameter on the stability conditions.

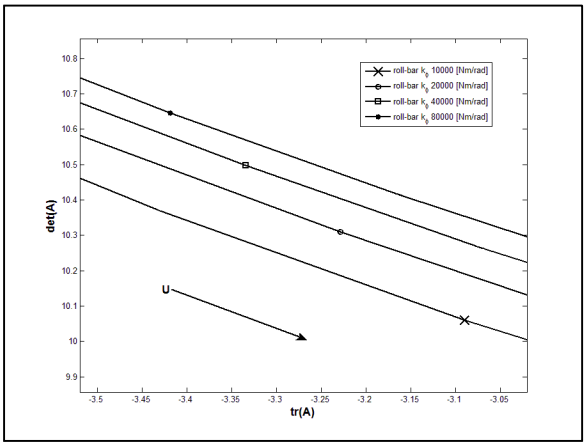

Fig. 4. Variations of the eigenvalues, expressed in terms of tr(A) and det(A), for a constant-steering curving manoeuvre, performed at increasing U, in conditions of stable equilibrium and for different values of the anti-roll stiffness.

It is possible to notice how, increasing longitudinal speed, the values of det(A) and of tr(A) tend to zero, thus approaching to unstable configuration. Employment of an adequately variable anti-roll stiffness sets the vehicle on more stable conditions, confirmed by higher values of det(A).

This last annotation could suggest the development of a controlled system, able to vary its anti-roll stiffness as a function of variables such as the longitudinal velocity or the lateral acceleration, with the purpose of increasing the stability of the vehicle.

As it concerns the vehicle handling behaviour, it can be interesting to examine the variations induced by different values of front anti-roll stiffness on the tyre slip angle (Milliken and Milliken, 1995).

Equipping an axle with an anti-roll bar influences the vehicle dynamics showing a decreasing roadholding of the axle for increasing values of the stiffness. Reducing the lateral force performed by the front axle can be useful, for an over-steering vehicle, to contrast this tendency, reducing, as a consequence, the rear axle slip angle.

Fig. 5 shows, using the same anti-roll stiffness adopted in Fig. 4, the left rear slip angle trend during the reference manoeuvre.

The different values of anti-roll stiffness employed in the simulations allow to evaluate its influence on vehicle stability and on rear slip angles: considering the reference manoeuvre, increasing the front anti-roll stiffness, the rear steady state slip angle values decrease; it means that controlling opportunely the anti-roll stiffness can contribute to reach a more stable configuration in comparison with the configuration obtained keeping constant values of stiffness.

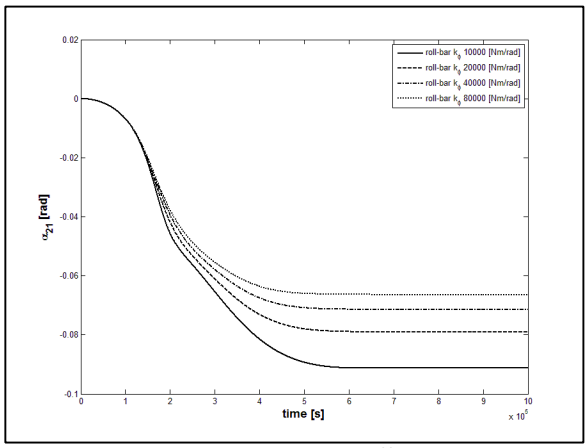

Fig. 5. Variations induced by different values of front axle anti-roll stiffness on the left rear slip angle.

5. The magnetorheological fluid anti-roll bar

The described results highlight that acting properly on the anti-roll stiffness of an axle it is possible to confer to the entire vehicle a more stable equilibrium configuration.

To this purpose, an innovative semi-active anti-roll bar, based on the properties of the magnetorheological fluids, will be now presented. The proposed idea allows to control the anti-roll stiffness of the axle on which it is installed, adopting the well known properties of the magnetorheological fluids, which are suitable for control-based applications.

The system is constituted by two parts: a passive one (A in Fig. 6), represented by a traditional torsional steel bar and a semi-active device B linked in parallel. The device B is characterized by the employment of magnetorheological fluid, thanks to which it is possible to regulate the stiffness.

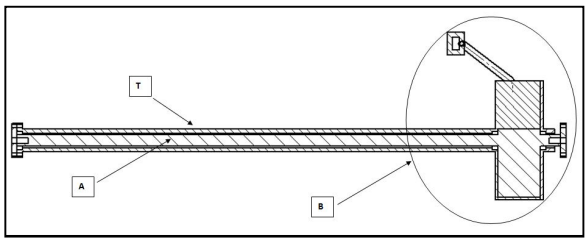

Figure 6: Section view of the magnetorheological fluid anti-roll bar. The passive part of the system, constituted by a high stiffness bar, is evidenced.

The device is constituted by an external cylindrical surface (C in Fig. 7) in which two elements (D1 and D2) are contained. The element D1 is integral with the classical anti-roll bar (A in Fig. 6), while element D2 is integral to the surface C. The surface C is made integral with the classical anti-roll bar by means of a coaxial pipe T characterized by a high value of torsional stiffness, so as to consider it as perfectly rigid.

Elements D1 and D2 are respectively integral with the two extreme sections of the classical anti-roll bar A. The elements D1 and D2, in relative motion, create two chambers E containing the magnetorheological fluid. The two chambers of the cylinder are connected by an external by-pass circuit (F in Fig. 7), characterized by a "virtual valve" G, that allows to control the equivalent torsional stiffness of the system. Particularly, by means of variation of the fluid magnetization, and then of its rheological properties, a regulation of the anti-roll stiffness can be produced. As an example, an increase in the magnetic field generates, as a consequence, an increase in fluid viscosity and an additional anti-roll torque acting on vehicle body.

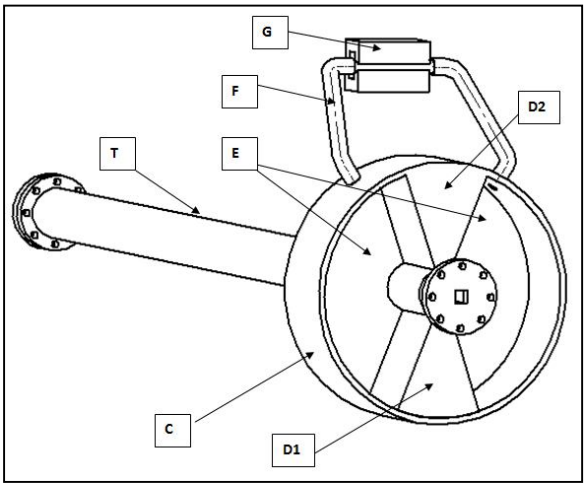

Figure 7: General scheme of the anti-roll bar. It is possible to distinguish the passive part, the chambers in which the fluid evolves and the external by-pass circuit.

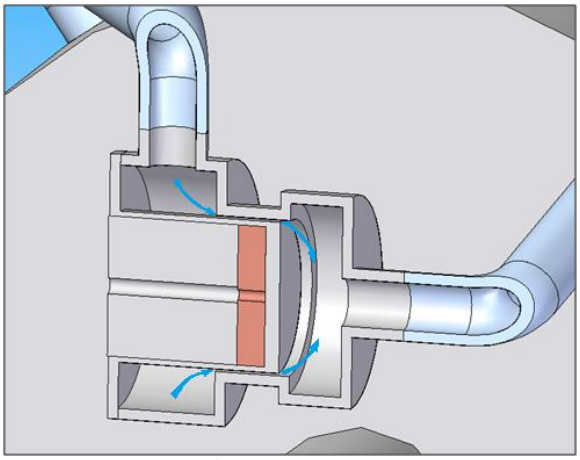

Figure 8: Scheme of the valve constituting the by-pass circuit. The fluid, passing through the coils following the blue arrows, is magnetized, changing its rheological properties.

In Fig. 8 it is showed the internal geometry of the virtual valve. It constrains the fluid, alternatively moving among the chambers through the pipes, to move across a circular-ring shaped section. The copper-coloured element represents the electric coils

generating the magnetic field, able to magnetize the fluid.

6. Semi-active anti-roll bar modelling

The pressure difference that takes place between the two volumes, generates the anti-roll torque ($M_{a\text{-}r}$). The last one, under the assumption of uncompressible fluid, can be written as:

$$M_{a-r} = (\Delta P + \Delta P_t)[(R_e - r_i)L_c]R_m \quad (16)$$

where

ΔP = pressure drop in the virtual valve (N/m^2);

ΔP_t = pressure drop in the by-pass pipeline (N/m^2);

R_e = cylinder outer radius (m);

r_i = cylinder inner radius (m);

L_c = cylinder height (m);

R_m = action mean radius (m).

The pressure drop in the by-pass pipeline is:

$$\Delta P_t = \frac{8\eta Q L_t}{\pi r_t^2} \quad (17)$$

where

η = fluid kinematic viscosity (m^2/s);

Q = flow rate (m^3/s);

L_t = length of the pipeline (m);

r_t = pipeline radius (m).

As regards the pressure drop in the virtual valve, it is given by the purely rheological component P_r and the magnetic field dependent (magneto-rheological) component P_{mr}, in accordance with the following (Phillips, 1969):

$$\Delta P = \Delta P_\eta + \Delta P_\tau = \frac{12\eta Q L_p}{g^3 w} + \frac{c\tau_y L_a}{g} \quad (18)$$

where

L_p is the length of the valve passive part (m);

w is the length of the medium circumference of the ring interested by the fluid flow (m);

g is the annular gap (m);

τ_y is the fluid yeld stress (N/m^2), dependent on the applied magnetic field;

L_a is the length of the valve semi-active part (m);

c is a characteristic fluid parameter (-);

For the sake of simplicity, pressure drops are hypothesized as independent by the flow direction of the by-pass circuit, and, in particular, of the virtual valve.
For the calculation of the volumetric circulation of the fluid evolving in the valve, starting from the fluid mass moved by a system unit rotation can be useful. Consequently, it will be:

$$m = \theta \frac{L_C(\pi R_e^2 - \pi r_i^2)}{360} \quad (19)$$

where:

m is the fluid mass moved by a bar unit rotation (kg);

θ is bar torsion angle (rad);

Deriving this equation it is possible to obtain the fluid flow rate:

$$Q = \dot{\theta} \frac{L_C(\pi R_e^2 - \pi r_i^2)}{360} \quad (20)$$

To this resistant torque is added the rate due to the passive bar, modeled as a torsion spring.

$$M_{passive} = K_\phi \theta \quad (21)$$

As a consequence the total resistant torque is:

$$M = M_{res} + M_{passive} \quad (22)$$

And the total equivalent stiffness can be evaluated as follows:

$$K_{\phi eq} = \frac{M}{\theta} \quad (23)$$

7. Conclusions

The purpose of the present paper is the study of the influence of the anti-roll stiffness on the local vehicle stability. To this aim, an 8 degrees-of-freedom quadricycle planar vehicle model has been employed. A reference manoeuvre has been chosen for this analysis: it is a curve approached with steering angle and longitudinal velocity both increasing to saturation values. The manoeuvre lasts until the steady state motion conditions are reached.

Tyre lateral forces, expressed by Pacejka's model, have been linearized for each tyre in the neighborhood of its equilibrium steady state point, to study local vehicle stability in the state space. This kind of analysis is characterized by a heavy

computational load, so it has been necessary to adopt simpler expressions of the lateral interaction forces, able, at the same time, to take into account the saturation phenomena due to lateral load transfers. The proposed linearized tyre model has been developed with the aim to satisfy these requirements.
The local stability analysis has been carried out, studying the eigenvalues of the motion equations system in the state space.
The results have been presented, highlighting the influence of the anti-roll stiffness of the axles on the local stability conditions, expressed by means of the state matrix A determinant and trace. It has been possible to notice how, varying adequately the anti-roll stiffness, a more stable equilibrium configuration is reachable.
As a consequence of this result, an innovative semi-active anti-roll bar has been described. This device is based on the properties of the magnetorheological fluids and is able to control the anti-roll stiffness of the axle on which it is installed, driving the vehicle to conditions of increased stability.

6. References

Escalona J. L., Chamorro R. 2007. *Stability analysis of vehicles on circular motions using multibody dynamics*, Nonlinear Dynamics, vol 53, 237-250.

Garetti S., Bittanti S. 2009. *Parameter Estimation in the Pacejka's Tyre Model through the TS Method*, 15th IFAC Symposium on System Identification.

Guiggiani M. 2007. *Dinamica del veicolo*, Città Studi Edizioni.

Milliken W. F., Milliken D. L. 1995. *Race Car Vehicle Dynamics*, SAE International.

Pacejka H. B. 2005. *Tire and Vehicle Dynamics*, SAE International.

Phillips R.W. 1969. *Engineering Applications of Fluids with a Variable Yield Stress*, Ph.D. Thesis.